Self-Organized Lane Formation in Bidirectional Transport by Molecular Motors

Robin Jose[*] and Ludger Santen[†]

Department of Theoretical Physics & Center for Biophysics, Saarland University,
66123 Saarbrücken, Germany

Within cells, vesicles and proteins are actively transported several micrometers along the cytoskeletal filaments. The transport along microtubules is propelled by dynein and kinesin motors, which carry the cargo in opposite directions. Bidirectional intracellular transport is performed with great efficiency, even under strong confinement, as for example in the axon. For this kind of transport system, one would expect generically cluster formation. In this Letter, we discuss the effect of the recently observed self-enhanced binding affinity along the kinesin trajectories on the microtubule. We introduce a stochastic lattice-gas model, where the enhanced binding affinity is realized via a floor field. From Monte Carlo simulations and a mean-field analysis we show that this mechanism can lead to self-organized symmetry breaking and lane formation that indeed leads to efficient bidirectional transport in narrow environments.

Introduction.—The efficiency of intracellular transport is one of the most intriguing features of biological cells. Different kinds of cellular cargo have to be transported to specific locations in order to maintain the cells' functionality. Intracellular transport can be driven by molecular motors, i.e., specialized proteins that can carry cargo along polar filaments of the cytoskeleton [1–4]. Molecular motors, such as the microtubule (MT) associated proteins (MAPS) kinesin and dynein, step stochastically along MTs in a given preferred direction: kinesins step typically toward the plus end and dyneins to the minus end. Molecular motors are able to carry big (on the scale of the cell) objects through crowded environments.

We focus on bidirectional motor-driven transport under spatial confinement, which is for example relevant for intracellular transport in axons. In this kind of environment, active transport is particularly difficult to organize, since cluster formation is generically observed in spatially extended one-dimensional systems [5–9]. Clusters can either have stationary particle output [7] or can lead to long times of blockages such as for non-Markovian site exchange [9]. The general question we address in this Letter is the following: how do confined systems of active particles self-organize to realize efficient bidirectional transport states?

Motor-driven transport has been described by variants of the totally asymmetric exclusion processes (TASEP), which combine the directed stochastic motion of particles on a one-dimensional lattice with hard-core exclusion and Langmuir-kinetics [5,10–12]. In principle, the particle exchange with a reservoir would allow for bidirectional transport, in case of large diffusivity of unbound particles. However, if the unbound particles are localized, so far no mechanism has been suggested which leads to efficient bidirectional transport. A rather direct approach is the self-organization in subsystems each of which carries unidirectional transport. A recent hypothesis is that post-translational modifications on MTs might organize transport in neurons [13,14]. This kind of organization has been observed for example in dendrites, where the MTs are oppositely oriented [15] and in MT doublets in cilia [16]. Furthermore, motor proteins can regulate MTs themselves [17], and MT dynamics [5] and tau [18] can affect motor transport.

Recent experimental findings suggest a possible mechanism leading to efficient bidirectional transport on MT bundles where no *a priori* compartmentalization exits. Shima *et al.* [19] reported that binding affinity of MTs for kinesin motors is self-enhanced along the kinesin trajectories which modify the MTs. This kind of self-induced preferential binding can be understood as a true realization of a floor field, which has been successfully introduced as a virtual mechanism in order to generate, e.g., lane formation in bidirectional pedestrian flows [20–24].

In this Letter, the transport problem is formulated as a TASEP with Langmuir-kinetics, where we additionally consider an explicit particle reservoir and a floor field. Our theoretical model describes the key features of bidirectional axonal transport but considerably reduces the complexity of the biological reference system.

The model.—We study a TASEP with Langmuir kinetics of two particle species moving on a pair of parallel, identically polarized one-dimensional filaments. The model filaments (MTs) are represented as one-dimensional, static lattices. Lattice sites can either be empty or occupied by a single particle. We consider two types of particles, i.e., moving to the plus end of the filament ($\tau = 1$, blue in Fig. 1) and to the minus end ($\tau = -1$, red).
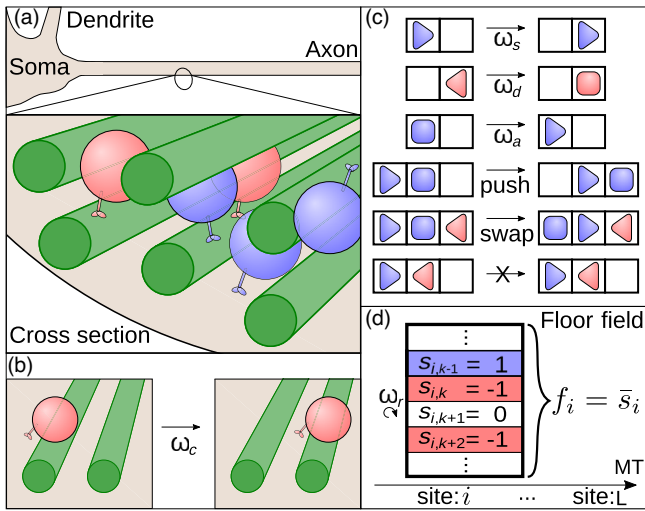
FIG. 1. (a) Scheme of a neuron, indicating the crowded environment and confinement inside axons, including MTs, plus particles (blue), and minus particles (red). (b) Unbound particles switch filaments with rate ω_c. (c) Particle dynamics in the exclusion process. Triangles mimic bound particles, the tip indicates the direction. Unbound particles are shown by squares. Bound particles can step or detach, unbound particles can reattach. If a particle attempts to step onto a site occupied by an unbound particle, it can either push it away or swap position. Two bound particles block each other via exclusion. (d) The floor-field state f_i is averaged over all substates for every site i of the lattice.

Particle dynamics: Both types of particles can either be bound or unbound to a filament [triangles or squares in Fig. 1(c)]. Bound particles step to the neighboring site (target site) with rate ω_s or detach from the filament with rate ω_d [Fig. 1(c)]. In order to study lane formation as a bulk effect, we are considering periodic boundary conditions. Particles which detach from the filament stay at the same lattice site, unlike in typical models with Langmuir kinetics where particles move to a bulk reservoir [5,11]. This feature is crucial for modeling transport in crowded environments, where unbound particles cannot simply diffuse away from clusters.

Unbound particles can reattach to the filament with rate ω_a or change to an unbound state on the other filament with a coupling rate ω_c [Fig. 1(b)], where the position is kept. Particles interact with each other via hardcore repulsion [Fig. 1(c), bottom]. We distinguish three cases for particles that are selected to step. (i) If the target site is free, the step is executed. (ii) If the target site is occupied by a bound particle the step is rejected. (iii) If the target site is occupied by an unbound particle, the unbound particle is either pushed to next site (in moving direction of the stepping particle) or exchanges position with it (swapping). If both pushing and swapping are possible, one of the two possibilities is selected with a probability of $1/2$. If the

site in moving direction next to the unbound particle is occupied, swapping is executed [Fig. 1(c)].

Floor-field dynamics: In [19,25] an axial elongation of the MT by kinesin has been reported. The elongation is related to a metastable tubulin state that has a higher binding affinity for kinesins. This effect is implemented via a floor field that considers the number of MT protofilaments, $N_p = 13$. A floor field f_i is assigned to each lattice site i, which is given by

$$f_i = \frac{1}{N_p} \sum_{k=1}^{N_p} s_{i,k}, \qquad (1)$$

where k denotes the index of the protofilament which is permanently assigned to the particles until they detach from the (proto-)filament. Therefore, f_i represents the average of N_p substates $s_{i,k} \in \{-1, 0, 1\}$. The value of f_i is updated if particle steps to site i and thereby sets the value of a given substate $s_{i,k}$ to $+1(-1)$ in case of $+(-)$ directed motors. The substate can decay back to 0 again with rate ω_r [Fig. 1(d)]. Averaging over N_p substates introduces a memory effect that stabilizes the preferential adsorption of a given type of particle, i.e., the amplitude of the floor field determines the robustness of the floor field against changes of the affinity by single oppositely directed particles. The subdivision of the floor field into "protofilaments" is also consistent with the observation that low kinesin concentration may lead to a curvature of MTs, which signifies a coexistence of excited and nonexited tubulin states [25].

The state f_i influences the binding affinity of particles $\omega_{a,i}$ given by

$$\omega_{a,i} = \begin{cases} \omega_a^0 \mu^{|f_i|}, & \tau = \mathrm{sgn}(f), \\ \omega_a^0 \frac{1}{\mu^{|f_i|}}, & \tau \neq \mathrm{sgn}(f), \end{cases} \qquad (2)$$

where ω_a^0 is the free attachment rate and $\mu \geq 1$ is called affinity modification factor. This modification leads to higher binding rates if the floor field state f_i was predominantly set by particles of the same type τ as well as lower rates for opposing combinations. If $\mu = 1$ or $f_i = 0$, the interaction is neutral. We consider a symmetric excitation for dynein and kinesin motors, though so far experimental evidence for a modification of the MT structure by dynein is still lacking.

Results and discussion.—We study the influence of the floor field on the particle flux J as a measure of transport efficiency as well as symmetry-breaking and self-organized lane formation. First, we introduce a mean-field analysis and then compare results to Monte Carlo (MC) simulations.

Mean-field analysis: As a reference, we consider TASEP models [26], two-species, bidirectional exclusion processes [7,9,27], as well as combinations of TASEP and Langmuir-kinetics [5,11,28]. From these models, a

mean-field estimation [29] of the flux $J_{\text{ud}} = \rho_{\text{eff}}(1 - \rho_{\text{eff}})$ can be deduced for unidirectional one-filament systems with Langmuir kinetics [30]. We use J_{ud} for judging on the transport efficiency. Note that fluxes are scaled by ω_s^{-1} and the system size L.

To include the floor-field dependency in a mean-field model, we assume a simplified unbound state (u) shared for both filaments called top (t) and bottom (b). The average floor field f is represented by the normalized difference in particle densities $\Delta_{t,+} = (\rho_t^+ - \rho_t^-)/\rho^+$ for the plus species and the top filament (bottom analog) so that we can formulate the mean-field equations exemplary for plus particles (details are in the Supplemental Material [30])

$$\frac{\partial \rho_t^+}{\partial t} = \omega_a^0 \mu^{\Delta_{t,+}} \rho_u^+ - \omega_d \rho_t^+,$$

$$\frac{\partial \rho_u^+}{\partial t} = \omega_d(\rho_t^+ + \rho_b^+) - (\mu^{\Delta_{t,+}} + \mu^{\Delta_{b,+}})\omega_a^0 \rho_u^+,$$

$$\frac{\partial \rho_b^+}{\partial t} = \omega_a^0 \mu^{\Delta_{b,+}} \rho_u^+ - \omega_d \rho_b^+. \tag{3}$$

Additionally, we get the identity $\rho^\pm = \rho_t^\pm + \rho_b^\pm + \rho_u^\pm$ from particle conservation. In the stationary state, we find the equation for the difference in densities on the top filament Δ as

$$\Delta = \frac{(\mu^\Delta - \mu^{-\Delta})}{\frac{1}{\omega_d}(\mu^\Delta + \mu^{-\Delta}) + \frac{\omega_d}{\omega_a^0}}. \tag{4}$$

Equation (4) is numerically solvable and shows a pitchfork bifurcation at a critical $\mu = \mu_{\text{crit}}$. For $\mu < \mu_{\text{crit}}$, Eq. (4) has only a single solution given by $\Delta_0 = 0$, while for $\mu > \mu_{\text{crit}}$ the solution $\Delta_0 = 0$ gets unstable and two stable points at $\Delta_\pm$, depending on ω_d and ω_a^0, occur. We also find that the floor field has to modify the affinity for both species, otherwise only a symmetric solution can be found [30].

By solving Eq. (4), the flux is estimated by

$$J_{\text{MF}} = \rho_t^+[1 - (\rho_t^+ + \rho_t^-)]. \tag{5}$$

Parameters: We used the experimental results of [19] to select the relevant parameters of the model, given in Table I in the Supplemental Material [30]. We kept the rates $\omega_s, \omega_d, \omega_a^0$, and ω_r constant. The relevant density regime is rather difficult to estimate. On the one hand the fraction of occupied binding sites is rather low. On the other hand molecular motors carry rather big objects (20 and 50 nm for axonal vesicles [32,33], compared to a 8-nm step size for most kinesin and dynein motors [34,35]), such that the density in terms of the occupied volume along the MT is considerably higher. Therefore, we did not focus on the low density regime of $\rho \approx 0.01$, which has been addressed in [19] but varied the particle density in order to study the stability of the bidirectional transport in our model.
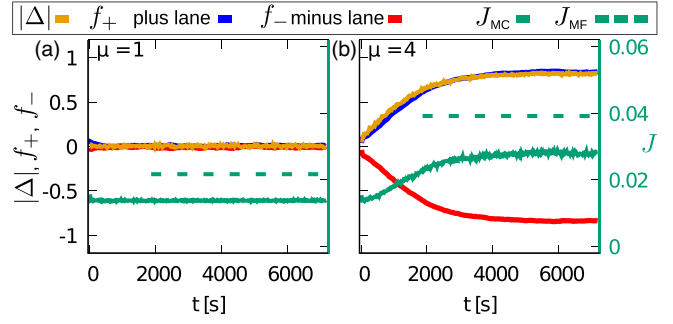

FIG. 2. Time dependence of the flux and particle densities for a system of $L = 1000$, $\rho = 0.05$, and random initial configurations. Values of the floor fields f_+, f_- and difference in densities Δ are given at the left axis; values of the total flux J, and the mean-field estimation J_{MF} are given at the right axis. (a) $\mu = 1$, (b) $\mu = 4$.

The chosen lengths of approximately 1000 sites, which correspond to MTs of length 8 μm, is in accordance to the typical MT length in axons [36,37]. The range of the affinity modification μ is motivated by different experiments in which kinesin binding affinity has been measured for different types of MTs. In [19,38], GTP-MTs show three to four times higher affinity than GDP-MTs and comparing [39] with [40], the affinity is five times higher. The choice of coupling rates, filament number and the number of sub-states in the floor-field implementation is discussed in the Supplemental Material [30].

MC simulations: We investigate the influence of the floor field on our stochastic model by performing MC simulations with two filaments started with neutral floor fields and randomly distributed particles. The total particle density is given by $\rho_{\text{tot}} = \rho_+ + \rho_- = 2\rho_+$.

A time-evolution of the system is shown in Fig. 2 averaged over 100 simulations. Yellow lines show the difference in densities Δ. A filament with average floor field $f = 1/L \sum_{i=1}^L f_i > 0$ is called plus lane and $f < 0$ minus lane. The floor field f_+ (f_-) of the plus (minus) lane is shown in blue (red), and the total flux J in green (right axis).

Without modification, i.e., $\mu = 1$ in Fig. 2(a), no symmetry breaking is observed. There is no significant difference between f_+ and f_-, and particles are distributed equally ($\Delta = 0$). By raising μ, the floor field values split up and Δ increases. For $\mu = 4$, f_+ (f_-) and Δ almost reach the extreme values ± 1, meaning a quasiseparation of particles and totally asymmetric floor fields. This lane formation is stable and the time evolution shows very little sample to sample fluctuations. Also the difference in the particle distribution Δ is in good agreement with the average floor field $|f|$ which makes Δ a good representation for f in the mean-field analysis.

The stationary flux (green) increases for higher μ when the floor-field is stabilized [Fig. 2(b) with $\mu = 4$]. In the case of $\mu = 4$ ($\mu = 6$), there is an average effective velocity
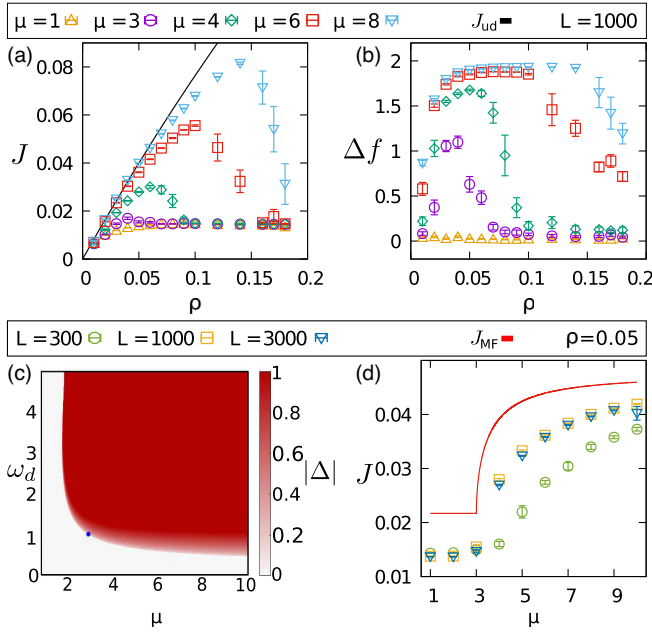
FIG. 3. Transport efficiency (a) and symmetry breaking [(b), (d)] under variation of density and affinity modification. Simulations did run for three hours real time, measurements started after one hour. Panel (c) shows the phase space for symmetric and asymmetric solutions in the mean-field model.

of ≈ 270 nm/s (350 nm/s) for a motor protein, whereas the free stepping velocity of bound kinesins is presumed to be 480 nm/s in this Letter [19]. As expected the mean-field solution (dashed green line in Fig. 2) overestimates the flux considerably, since a homogeneous distribution of particles is assumed, while in the full model there are strong density correlations due to cluster formation. However, the initially symmetric two-lane system spontaneously breaks symmetry so both lanes carry stationary and oppositely directed net flows.

In Fig. 3(a), we show the density dependence of the flux for different μ in comparison to the unidirectional flux. Simulation results show that the transport efficiency of the system is significantly increased for ($\mu \geq 3$) compared to the plateau obtained without a floor field ($\mu = 1$). Actually, the flux reaches almost the value of the corresponding unidirectional flux to J_{ud} until it breaks down to the traffic jam plateau value, similar for all μ. The density at which the transition to the plateau value is observed depends on μ. Note that the stationary state is not always reached at high densities if we initialize the system with a random configuration, indicated by the larger error bars in the high density regime caused by metastable clusters [Fig. 3(a)], which have not been dissolved within the simulation time.

Lane formation is both well characterized by the difference in floor fields $\Delta f = f_+ - f_-$ measuring asymmetry between filaments and is shown in Fig. 3(b). The base line corresponds to symmetric fields without lane formation for $\mu = 1$. By increasing μ, the asymmetry develops in a density dependent range before Δf drops down. Results of Figs. 3(a) and 3(b) indicate a lane formation and quasiordering of the system into two subsystems with oppositely directed flux. When the self-organization breaks down, traffic jams are forming on both lanes and transport efficiency is not enhanced anymore. This is consistent with lane formation observed in other floor-field models [20].

The influence of μ on the symmetry-breaking is further examined in Figs. 3(c) and 3(d) by comparing mean-field results to MC simulations. In Fig. 3(c), a phase diagram from mean-field analysis for $|\Delta|$ under variation of μ and ω_d is shown for fixed $\omega_a^0 = 5$ s^{-1}. The blue dot marks μ_{crit} for ω_d used in simulations and agrees with Figs. 2 and 3(b). The border of $|\Delta| > 0$ shows that $\mu_{\mathrm{crit}} > 1$ for arbitrary ω_d. There is only a small region where $0 < |\Delta| < 1$ because the mathematical solution of Eq. (4) can be larger than the physical border of $|\Delta| = 1$, hence particles are completely separated. The transition is sharper for shorter run lengths (larger ω_d). In Fig. 3(d), J is growing under variation of μ for constant $\rho = 0.05$ and different L. Remarkably, the transition from a symmetric to a stable asymmetric solution is captured by the mean-field approach and even the predicted value μ_{crit} agrees well with simulation results. The transition is sharper for $L \geq 1000$ than for $L = 300$, hence, the larger system is better approximated by the mean-field model. Also, larger systems have higher fluxes. This is in contrast to the plateau value for $\mu = 1$, which decreases with the system size. For even larger L it is computationally hard to achieve stationary states but we expect the system to still self-organize in lanes due to stable lanes if already started in such conditions [30].

Conclusion and outlook.—To summarize, we introduced a stable mechanism for efficient bidirectional transport of active particles in one-dimensional systems under strong confinement. This mechanism is based on self-organized lane formation. Directed lanes may be predefined in engineered systems, however, this is not always the case for transport of animals or humans as for instance in pedestrian dynamics where self-organized lane formation occurs [20–24]. The influence of the floor field on particle binding was inspired by recent experimental results on self-induced strengthening of the kinesin MT affinity, but could also be realized by other modifications of MTs. Lane formation can be captured by a mean-field approach, which shows the mechanism is stable against local density fluctuations.

The stability of lane formation is remarkable in several respects. First of all, lane formation is observed in the biologically relevant low density regime. This is in contrast to other mechanisms, based on particle-particle interactions [41], which lead to symmetry breaking at high densities and therefore low particle velocities, while *in vivo* observations of, e.g., axonal vesicle transport show that vesicles transported by molecular motors reach the free stepping

velocities of kinesin. Second, we observe the coexistence of transport in both directions on a coupled pair of filaments, which goes beyond symmetry-breaking mechanisms reported as discussed in, e.g., [42] where symmetry breaking leads to unidirectional transport. Third, our model describes the low mobility of unbound particles, which may trigger cluster formation in bidirectional transport and illustrates the stability of the suggested mechanism. From our point of view, our results indicate that stable bidirectional flows are more easily realized by modifications of the filaments rather than interactions between particles.

The importance of the MT structure on transport has recently been pointed out [13–16]. Bidirectional intracellular transport is organized on oppositely oriented filament bundles in dendrites [15] and on parallel oriented MT doublets in cilia [16]. In axons, however, so far a similar organization of the MT network has not been identified. Our findings indicate that the post-translational modification by motors and self-induced preferential binding of one or the other motor species could indeed lead to stable bidirectional transport in an *a prior* unipolar MT network. A self-induced amplification of the binding affinity must be given for both particle species. Otherwise, the density of oppositely oriented particles on the same filament is too high to realize efficient transport states.

Concerning the robustness and efficiency of the proposed lane formation in our model for intracellular transport, it would be of great interest to obtain further insight to the interplay between dynein and kinesin motors, microtubules, and MAPS, which might have a strong impact on the (self-)organization of intracellular transport.

---

[*]rjose@lusi.uni-sb.de

[†]l.santen@mx.uni-saarland.de

[1] N. Hirokawa and R. Takemura, Nat. Rev. Neurosci. **6**, 201 (2005).

[2] A. Brown, J. Cell Biol. **160**, 817 (2003).

[3] C. Herold, C. Leduc, R. Stock, S. Diez, and P. Schwille, ChemPhysChem **13**, 1001 (2012).

[4] P. J. Hollenbeck and W. M. Saxton, J. Cell Sci. **118**, 5411 (2005).

[5] M. Ebbinghaus, C. Appert-Rolland, and L. Santen, J. Stat. Mech. (2011) P07004.

[6] C. Appert-Rolland, M. Ebbinghaus, and L. Santen, Phys. Rep. **593**, 1 (2015).

[7] M. Evans, D. Foster, C. Godrèche, and D. Mukamel, J. Stat. Phys. **80**, 69 (1995).

[8] G. Korniss, B. Schmittmann, and R. Zia, Europhys. Lett. **45**, 431 (1999).

[9] R. Jose, C. Arita, and L. Santen, J. Stat. Mech. (2020) 033207.

[10] A. Parmeggiani, T. Franosch, and E. Frey, Phys. Rev. Lett. **90**, 086601 (2003).

[11] A. Parmeggiani, T. Franosch, and E. Frey, Phys. Rev. E **70**, 046101 (2004).

[12] I. Pinkoviezky and N. S. Gov, Phys. Rev. Lett. **118**, 018102 (2017).

[13] S. Gadadhar, S. Bodakuntla, K. Natarajan, and C. Janke, J. Cell Sci. **130**, 1347 (2017).

[14] C. Janke, J. Cell Biol. **206**, 461 (2014).

[15] R. P. Tas, A. Chazeau, B. M. C. Cloin, M. L. A. Lambers, C. C. Hoogenraad, and L. C. Kapitein, Neuron **96**, 1264 (2017).

[16] L. Stepanek and G. Pigino, Science **352**, 721 (2016).

[17] D. Johann, C. Erlenkämper, and K. Kruse, Phys. Rev. Lett. **108**, 258103 (2012).

[18] A. Ebneth, R. Godemann, K. Stamer, S. Illenberger, B. Trinczek, E.-M. Mandelkow, and E. Mandelkow, J. Cell Biol. **143**, 777 (1998).

[19] T. Shima, M. Morikawa, J. Kaneshiro, T. Kambara, S. Kamimura, T. Yagi, H. Iwamoto, S. Uemura, H. Shigematsu, and M. Shirouzu, J. Cell Biol. **217**, 4164 (2018).

[20] C. Burstedde, K. Klauck, A. Schadschneider, and J. Zittartz, Physica (Amsterdam) **295A**, 507 (2001).

[21] S. Nowak and A. Schadschneider, Phys. Rev. E **85**, 066128 (2012).

[22] M. Chraibi, A. Tordeux, A. Schadschneider, and A. Seyfried, in *Complex Dynamics of Traffic Management* (Springer US, New York, NY, 2019), pp. 649–669.

[23] L. Gibelli and N. Bellomo, *Crowd Dynamics, Volume 1: Theory, Models, and Safety Problems* (Springer, Basel, 2019).

[24] A. Schadschneider, D. Chowdhury, and K. Nishinari, *Stochastic Transport in Complex Systems: From Molecules to Vehicles* (Elsevier, Amsterdam, 2010).

[25] D. Peet, N. Burroughs, and R. Cross, Nat. Nanotechnol. 1 **13**, 386 (2018).

[26] B. Derrida, Phys. Rep. **301**, 65 (1998).

[27] P. Arndt, T. Heinzel, and V. Rittenberg, J. Phys. A **31**, L45 (1998).

[28] M. Ebbinghaus and L. Santen, J. Stat. Mech. (2009) P03030.

[29] M. R. Evans, R. Juhász, and L. Santen, Phys. Rev. E **68**, 026117 (2003).

[30] See the Supplemental Material at http://link.aps.org/supplemental/10.1103/PhysRevLett.124.198103 for the set of parameters, a detailed mean-field analysis, and a discussion of the used reference set, which includes Ref. [31].

[31] T. Reichenbach, E. Frey, and T. Franosch, New J. Phys. **9**, 159 (2007).

[32] K. Harris and P. Sultan, Neuropharmacology **34**, 1387 (1995).

[33] D. Hall and E. Hedgecock, Cell **65**, 837 (1991).

[34] K. Svoboda, C. Schmidt, B. Schnapp, and S. Block, Nature (London) **365**, 721 (1993).

[35] E. Hirakawa, H. Higuchi, and Y. Toyoshima, Proc. Natl. Acad. Sci. U.S.A. **97**, 2533 (2000).

[36] M. R. Shaebani, A. Pasula, A. Ott, and L. Santen, Sci. Rep. **6**, 30285 (2016).

[37] W. Yu and P. Baas, J. Neurosci. **14**, 2818 (1994).

[38] M. Morikawa, H. Yajima, R. Nitta, S. Inoue, T. Ogura, C. Sato, and N. Hirokawa, EMBO J. **34**, 1270 (2015).

[39] S. Rosenfeld, B. Rener, J. Correia, M. Mayo, and H. Cheung, J. Biol. Chem. **271**, 9473 (1996).

[40] T. Nakata, S. Niwa, Y. Okada, F. Perez, and N. Hirokawa, J. Cell Biol. **194**, 245 (2011).

[41] S. Klumpp and R. Lipowsky, Europhys. Lett. **66**, 90 (2004).

[42] V. Popkov and I. Peschel, Phys. Rev. E **64**, 026126 (2001).